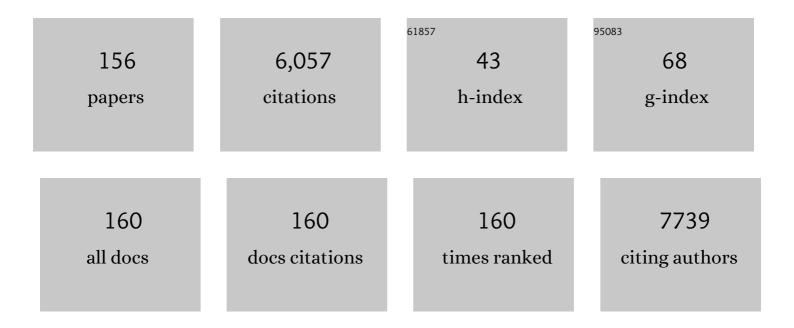
List of Publications by Year in descending order

Source: https://exaly.com/author-pdf/917792/publications.pdf Version: 2024-02-01



YUN CHEN

#	Article	IF	CITATIONS
1	Hydroxypropyl Chitosan/Soy Protein Isolate Conduits Promote Peripheral Nerve Regeneration. Tissue Engineering - Part A, 2022, 28, 225-238.	1.6	5
2	Oriented nanofibrous P(MMD-co-LA)/Deferoxamine nerve scaffold facilitates peripheral nerve regeneration by regulating macrophage phenotype and revascularization. Biomaterials, 2022, 280, 121288.	5.7	46
3	Multifunctional Double‣ayer Composite Hydrogel Conduit Based on Chitosan for Peripheral Nerve Repairing. Advanced Healthcare Materials, 2022, 11, e2200115.	3.9	34
4	A Hydrogen Bonds-Crosslinked Hydrogels With Self-Healing and Adhesive Properties for Hemostatic. Frontiers in Bioengineering and Biotechnology, 2022, 10, 855013.	2.0	23
5	Secretome of Mesenchymal Stem Cells from Consecutive Hypoxic Cultures Promotes Resolution of Lung Inflammation by Reprogramming Anti-Inflammatory Macrophages. International Journal of Molecular Sciences, 2022, 23, 4333.	1.8	5
6	Arbitrarily shapeable and conductive hydrogel with "Magic Cube―like structure for real-time monitoring and promoting wound healing. Composites Part B: Engineering, 2022, 238, 109903.	5.9	18
7	Mussel-inspired multifunctional surface through promoting osteogenesis and inhibiting osteoclastogenesis to facilitate bone regeneration. Npj Regenerative Medicine, 2022, 7, 29.	2.5	19
8	Self-Healing Hyaluronic Acid Nanocomposite Hydrogels with Platelet-Rich Plasma Impregnated for Skin Regeneration. ACS Nano, 2022, 16, 11346-11359.	7.3	70
9	Fabrication of Hydroxypropyl Chitosan/Soy Protein Isolate Hydrogel for Effective Hemorrhage Control. Tissue Engineering - Part A, 2021, 27, 788-795.	1.6	16
10	Hypoxic Preconditioning Enhances the Efficacy of Mesenchymal Stem Cells-Derived Conditioned Medium in Switching Microglia toward Anti-inflammatory Polarization in Ischemia/Reperfusion. Cellular and Molecular Neurobiology, 2021, 41, 505-524.	1.7	35
11	Green fabrication of seedbed-like Flammulina velutipes polysaccharides–derived scaffolds accelerating full-thickness skin wound healing accompanied by hair follicle regeneration. International Journal of Biological Macromolecules, 2021, 167, 117-129.	3.6	16
12	Electrofabrication of flexible and mechanically strong tubular chitosan implants for peripheral nerve regeneration. Journal of Materials Chemistry B, 2021, 9, 5537-5546.	2.9	15
13	Facile fabrication of soy protein isolate-functionalized nanofibers with enhanced biocompatibility and hemostatic effect on full-thickness skin injury. Nanoscale, 2021, 13, 15743-15754.	2.8	17
14	Topological defects of integer charge in cell monolayers. Soft Matter, 2021, 17, 5878-5887.	1.2	25
15	Structure of an activated DNA-PK and its implications for NHEJ. Molecular Cell, 2021, 81, 801-810.e3.	4.5	77
16	Mechanical stimulation enhances development of scaffoldâ€free, 3Dâ€printed, engineered heart tissue grafts. Journal of Tissue Engineering and Regenerative Medicine, 2021, 15, 503-512.	1.3	14
17	Conductive Hydroxyethyl Cellulose/Soy Protein Isolate/Polyaniline Scaffolds Promote PC12 Cells Neurite Elongation and BDNF Expression under Electrical Stimulation. Biomedical and Health Research, 2021, , .	0.0	1
18	Ultrafast Fabrication of Self-Healing and Injectable Carboxymethyl Chitosan Hydrogel Dressing for Wound Healing. ACS Applied Materials & Interfaces, 2021, 13, 24095-24105.	4.0	126

YUN CHEN

#	Article	IF	CITATIONS
19	Nanowire Assisted Mechanotyping of Cellular Metastatic Potential. Advanced Functional Materials, 2021, 31, 2101638.	7.8	3
20	Bacteria induce skin regeneration via IL- $1\hat{l}^2$ signaling. Cell Host and Microbe, 2021, 29, 777-791.e6.	5.1	78
21	Construction of conductive hydroxyethyl cellulose/soy protein isolate/polypyrrole composite sponges and their performances. Cellulose, 2021, 28, 8527-8539.	2.4	1
22	Parametric comparison between sparsity-based and deep learning-based image reconstruction of super-resolution fluorescence microscopy. Biomedical Optics Express, 2021, 12, 5246.	1.5	4
23	Natural <i>Flammulina velutipes</i> -Based Nerve Guidance Conduit as a Potential Biomaterial for Peripheral Nerve Regeneration: In Vitro and In Vivo Studies. ACS Biomaterials Science and Engineering, 2021, 7, 3821-3834.	2.6	13
24	IL-17F depletion accelerates chitosan conduit guided peripheral nerve regeneration. Acta Neuropathologica Communications, 2021, 9, 125.	2.4	4
25	A novel human endometrial epithelial cell line for modeling gynecological diseases and for drug screening. Laboratory Investigation, 2021, 101, 1505-1512.	1.7	9
26	Bioinspired Redwoodâ€Like Scaffolds Coordinated by In Situâ€Generated Silicaâ€Containing Hybrid Nanocoatings Promote Angiogenesis and Osteogenesis both In Vitro and In Vivo. Advanced Healthcare Materials, 2021, 10, e2101591.	3.9	19
27	Preparation of hydroxybutyl starch with a high degree of substitution and its application in temperature-sensitive hydrogels. Food Chemistry, 2021, 355, 129472.	4.2	20
28	Comprehensive strategy of conduit guidance combined with VEGF producing Schwann cells accelerates peripheral nerve repair. Bioactive Materials, 2021, 6, 3515-3527.	8.6	44
29	Effect of the Degree of Acetylation of Chitin Nonwoven Fabrics for Promoting Wound Healing. ACS Applied Bio Materials, 2021, 4, 1833-1842.	2.3	17
30	Ordered assembly of the cytosolic RNA-sensing MDA5-MAVS signaling complex via binding to unanchored K63-linked poly-ubiquitin chains. Immunity, 2021, 54, 2218-2230.e5.	6.6	23
31	Conductive, Self-Healing, Adhesive, and Antibacterial Hydrogels Based on Lignin/Cellulose for Rapid MRSA-Infected Wound Repairing. ACS Applied Materials & Interfaces, 2021, 13, 52333-52345.	4.0	68
32	Preparation and properties of granular cold-water-soluble porous starch. International Journal of Biological Macromolecules, 2020, 144, 656-662.	3.6	35
33	Early Vascular Cells Improve Microvascularization Within 3D Cardiac Spheroids. Tissue Engineering - Part C: Methods, 2020, 26, 80-90.	1.1	21
34	Conductive Hydroxyethyl Cellulose/Soy Protein Isolate/Polyaniline Conduits for Enhancing Peripheral Nerve Regeneration via Electrical Stimulation. Frontiers in Bioengineering and Biotechnology, 2020, 8, 709.	2.0	30
35	Elevated Extracellular Fluid Viscosity Stimulates Migration of Metastatic Cancer Cells. Biophysical Journal, 2020, 118, 602a.	0.2	1
36	A biodegradable soy protein isolate-based waterborne polyurethane composite sponge for implantable tissue engineering. Journal of Materials Science: Materials in Medicine, 2020, 31, 120.	1.7	11

#	Article	IF	CITATIONS
37	Biomimetic mineralization of novel hydroxyethyl cellulose/soy protein isolate scaffolds promote bone regeneration in vitro and in vivo. International Journal of Biological Macromolecules, 2020, 162, 1627-1641.	3.6	54
38	Cancer cells display increased migration and deformability in pace with metastatic progression. FASEB Journal, 2020, 34, 9307-9315.	0.2	33
39	Brain Derived Neurotrophic Factor and Glial Cell Line-Derived Neurotrophic Factor-Transfected Bone Mesenchymal Stem Cells for the Repair of Periphery Nerve Injury. Frontiers in Bioengineering and Biotechnology, 2020, 8, 874.	2.0	16
40	Stretching DNA origami: effect of nicks and Holliday junctions on the axial stiffness. Nucleic Acids Research, 2020, 48, 12407-12414.	6.5	7
41	Force-dependent trans-endocytosis by breast cancer cells depletes costimulatory receptor CD80 and attenuates T cell activation. Biosensors and Bioelectronics, 2020, 165, 112389.	5.3	11
42	Multiscale brain research on a microfluidic chip. Lab on A Chip, 2020, 20, 1531-1543.	3.1	20
43	Force-dependent extracellular matrix remodeling by early-stage cancer cells alters diffusion and induces carcinoma-associated fibroblasts. Biomaterials, 2020, 234, 119756.	5.7	44
44	Bioinspired Materials with Selfâ€Adaptable Mechanical Properties. Advanced Materials, 2020, 32, e1906970.	11.1	49
45	The Effects of Stiffness, Fluid Viscosity, and Geometry of Microenvironment in Homeostasis, Aging, and Diseases: A Brief Review. Journal of Biomechanical Engineering, 2020, 142, .	0.6	24
46	Characterization of Bone Marrow and Wharton's Jelly Mesenchymal Stromal Cells Response on Multilayer Braided Silk and Silk/PLCL Scaffolds for Ligament Tissue Engineering. Polymers, 2020, 12, 2163.	2.0	8
47	Intracellular pathway of halloysite nanotubes: potential application for antitumor drug delivery. Journal of Materials Science, 2019, 54, 693-704.	1.7	27
48	Cell–Cell Adhesion and Myosin Activity Regulate Cortical Actin Assembly in Mammary Gland Epithelium on Concaved Surface. Cells, 2019, 8, 813.	1.8	6
49	Electroassembly of Chitin Nanoparticles to Construct Freestanding Hydrogels and High Porous Aerogels for Wound Healing. ACS Applied Materials & Interfaces, 2019, 11, 34766-34776.	4.0	46
50	An implantable and versatile piezoresistive sensor for the monitoring of human–machine interface interface interactions and the dynamical process of nerve repair. Nanoscale, 2019, 11, 21103-21118.	2.8	44
51	Emerging chitin nanogels/rectorite nanocomposites for safe and effective hemorrhage control. Journal of Materials Chemistry B, 2019, 7, 5096-5103.	2.9	30
52	Starch Nanoparticles–Graphene Aerogels with High Supercapacitor Performance and Efficient Adsorption. ACS Sustainable Chemistry and Engineering, 2019, 7, 14064-14073.	3.2	68
53	Shape memory histocompatible and biodegradable sponges for subcutaneous defect filling and repair: greatly reducing surgical incision. Journal of Materials Chemistry B, 2019, 7, 5848-5860.	2.9	23
54	Versatile and High-throughput Force Measurement Platform for Dorsal Cell Mechanics. Scientific Reports, 2019, 9, 13286.	1.6	8

#	Article	IF	CITATIONS
55	An Economic, Modular, and Portable Skin Viscoelasticity Measurement Device for In Situ Longitudinal Studies. Molecules, 2019, 24, 907.	1.7	19
56	Myosin II governs intracellular pressure and traction by distinct tropomyosin-dependent mechanisms. Molecular Biology of the Cell, 2019, 30, 1170-1181.	0.9	27
57	The small GTPase RhoG regulates microtubule-mediated focal adhesion disassembly. Scientific Reports, 2019, 9, 5163.	1.6	10
58	Bone marrow mesenchymal stem cellsâ€derived conditioned medium protects cardiomyocytes from hypoxia/reoxygenationâ€induced injury through Notch2/mTOR/autophagy signaling. Journal of Cellular Physiology, 2019, 234, 18906-18916.	2.0	22
59	Response of collagen matrices under pressure and hydraulic resistance in hydrogels. Soft Matter, 2019, 15, 2617-2626.	1.2	14
60	A simple mechanical agitation method to fabricate chitin nanogels directly from chitin solution and subsequent surface modification. Journal of Materials Chemistry B, 2019, 7, 2226-2232.	2.9	9
61	Preparation and emulsification properties of dialdehyde starch nanoparticles. Food Chemistry, 2019, 286, 467-474.	4.2	59
62	Construction of highly biocompatible hydroxyethyl cellulose/soy protein isolate composite sponges for tissue engineering. Chemical Engineering Journal, 2018, 341, 402-413.	6.6	35
63	Design of bright near-infrared-emitting quantum dots capped with different stabilizing ligands for tumor targeting. RSC Advances, 2018, 8, 4221-4229.	1.7	8
64	Electrodeposition to construct mechanically robust chitosan-based multi-channel conduits. Colloids and Surfaces B: Biointerfaces, 2018, 163, 412-418.	2.5	17
65	Digestibility and physicochemical properties of starch-galactomannan complexes by heat-moisture treatment. Food Hydrocolloids, 2018, 77, 853-862.	5.6	28
66	3D-printed magnetic tweezers for dorsal traction force measurement. BioTechniques, 2018, 65, 347-349.	0.8	4
67	Dynamic adhesion characterization of cancer cells under blood flow-mimetic conditions: effects of cell shape and orientation on drag force. Microfluidics and Nanofluidics, 2018, 22, 1.	1.0	3
68	Mechanical Characterization of hiPSCâ€Derived Cardiac Tissues for Quality Control. Advanced Biology, 2018, 2, 1800251.	3.0	6
69	Mesenchymal stem cell interacted with PLCL braided scaffold coated with polyâ€< scp>lâ€lysine/hyaluronic acid for ligament tissue engineering. Journal of Biomedical Materials Research - Part A, 2018, 106, 3042-3052.	2.1	17
70	Accelerated skin wound healing by soy protein isolate–modified hydroxypropyl chitosan composite films. International Journal of Biological Macromolecules, 2018, 118, 1293-1302.	3.6	61
71	Electrical Writing onto a Dynamically Responsive Polysaccharide Medium: Patterning Structure and Function into a Reconfigurable Medium. Advanced Functional Materials, 2018, 28, 1803139.	7.8	27
72	Computer-Aided Laser Dissection: A Microdissection Workflow Leveraging Image Analysis Tools. Journal of Pathology Informatics, 2018, 9, 45.	0.8	10

#	Article	IF	CITATIONS
73	Is there a cause-and-effect relationship between physicochemical properties and cell behavior of alginate-based hydrogel obtained after sterilization?. Journal of the Mechanical Behavior of Biomedical Materials, 2017, 68, 134-143.	1.5	15
74	Kinetics of milk lipid droplet transport, growth, and secretion revealed by intravital imaging: lipid droplet release is intermittently stimulated by oxytocin. Molecular Biology of the Cell, 2017, 28, 935-946.	0.9	68
75	Advance of DNA and CCPs-based nanocarriers in drug delivery systems. Bio-Medical Materials and Engineering, 2017, 28, S255-S261.	0.4	2
76	Improvement of functionality after chitosan-modified zein biocomposites. Journal of Biomaterials Science, Polymer Edition, 2017, 28, 227-239.	1.9	13
77	Concerted actions of distinct nonmuscle myosin II isoforms drive intracellular membrane remodeling in live animals. Journal of Cell Biology, 2017, 216, 1925-1936.	2.3	52
78	Long-term antibacterial protected cotton fabric coating by controlled release of chlorhexidine gluconate from halloysite nanotubes. RSC Advances, 2017, 7, 18917-18925.	1.7	29
79	Comparison of MSC properties in two different hydrogels. Impact of mechanical properties. Bio-Medical Materials and Engineering, 2017, 28, S193-S200.	0.4	10
80	Rat BMSC infusion was unable to ameliorate inflammatory injuries in tissues of mice with LPS-induced endotoxemia. Bio-Medical Materials and Engineering, 2017, 28, S129-S138.	0.4	7
81	Electrodeposition to construct free-standing chitosan/layered double hydroxides hydro-membrane for electrically triggered protein release. Colloids and Surfaces B: Biointerfaces, 2017, 158, 474-479.	2.5	21
82	Enhanced Peripheral Nerve Regeneration by a High Surface Area to Volume Ratio of Nerve Conduits Fabricated from Hydroxyethyl Cellulose/Soy Protein Composite Sponges. ACS Omega, 2017, 2, 7471-7481.	1.6	29
83	Graphene oxide-modified electrospun polyvinyl alcohol nanofibrous scaffolds with potential as skin wound dressings. RSC Advances, 2017, 7, 28826-28836.	1.7	54
84	High-Throughput Microdissection for Next-Generation Sequencing. PLoS ONE, 2016, 11, e0151775.	1.1	21
85	Environmental Risk Factors in Han and Uyghur Children with Dyslexia: A Comparative Study. PLoS ONE, 2016, 11, e0159042.	1.1	20
86	Strong and Rapidly Selfâ€Healing Hydrogels: Potential Hemostatic Materials. Advanced Healthcare Materials, 2016, 5, 2813-2822.	3.9	138
87	Cellulose/soy protein composite-based nerve guidance conduits with designed microstructure for peripheral nerve regeneration. Journal of Neural Engineering, 2016, 13, 056019.	1.8	21
88	Construction of biocompatible regenerated cellulose/SPI composite beads using high-voltage electrostatic technique. RSC Advances, 2016, 6, 52528-52538.	1.7	10
89	Improved Mechanical Properties and Sustained Release Behavior of Cationic Cellulose Nanocrystals Reinforeced Cationic Cellulose Injectable Hydrogels. Biomacromolecules, 2016, 17, 2839-2848.	2.6	87
90	Controlled delivery of platelet-derived growth factor-BB from injectable microsphere/hydrogel composites. Colloids and Surfaces B: Biointerfaces, 2016, 148, 308-316.	2.5	8

#	Article	IF	CITATIONS
91	Hydrogels: Strong and Rapidly Self-Healing Hydrogels: Potential Hemostatic Materials (Adv.) Tj ETQq1 1 0.78431	4 rgBT	/Overgock 10 Th
92	Epichlorohydrin-Cross-linked Hydroxyethyl Cellulose/Soy Protein Isolate Composite Films as Biocompatible and Biodegradable Implants for Tissue Engineering. ACS Applied Materials & Interfaces, 2016, 8, 2781-2795.	4.0	120
93	Soy protein-modified waterborne polyurethane biocomposites with improved functionality. RSC Advances, 2016, 6, 12837-12849.	1.7	5
94	Reinforced Mechanical Properties and Tunable Biodegradability in Nanoporous Cellulose Gels: Poly(<scp>l</scp> -lactide- <i>co</i> -caprolactone) Nanocomposites. Biomacromolecules, 2016, 17, 1506-1515.	2.6	32
95	Improvement in physical and biological properties of chitosan/soy protein films by surface grafted heparin. International Journal of Biological Macromolecules, 2016, 83, 19-29.	3.6	38
96	Construction of nerve guide conduits from cellulose/soy protein composite membranes combined with Schwann cells and pyrroloquinoline quinone for the repair of peripheral nerve defect. Biochemical and Biophysical Research Communications, 2015, 457, 507-513.	1.0	48
97	Structure, physical properties, hemocompatibility and cytocompatibility of starch/zein composites. Bio-Medical Materials and Engineering, 2015, 25, 47-55.	0.4	5
98	Cellulose/soy protein isolate composite membranes: Evaluations of in vitro cytocompatibility with Schwann cells and in vivo toxicity to animals. Bio-Medical Materials and Engineering, 2015, 25, 57-64.	0.4	6
99	Abstract 230: Do-It-Yourself expression microdissection (DIY xMD): A low-cost, high-throughput cell and organelle isolation system. , 2015, , .		0
100	InÂVivo Tissue-wide Synchronization of Mitochondrial Metabolic Oscillations. Cell Reports, 2014, 9, 514-521.	2.9	38
101	Fabrication and evaluation of physical properties and cytotoxicity of zein-based polyurethanes. Journal of Materials Science: Materials in Medicine, 2014, 25, 823-833.	1.7	12
102	Construction of Chitin/PVA Composite Hydrogels with Jellyfish Gel-Like Structure and Their Biocompatibility. Biomacromolecules, 2014, 15, 3358-3365.	2.6	101
103	Fast Contact of Solid–Liquid Interface Created High Strength Multi-Layered Cellulose Hydrogels with Controllable Size. ACS Applied Materials & Interfaces, 2014, 6, 1872-1878.	4.0	87
104	Super-Suppression of Mitochondrial Reactive Oxygen Species Signaling Impairs Compensatory Autophagy in Primary Mitophagic Cardiomyopathy. Circulation Research, 2014, 115, 348-353.	2.0	163
105	Wireless Amplified Nuclear MR Detector (WAND) for High-Spatial-Resolution MR Imaging of Internal Organs: Preclinical Demonstration in a Rodent Model. Radiology, 2013, 268, 228-236.	3.6	38
106	Preparation of poly(sebacic anhydride) and polylactic acid pills used as drug carrier for levofloxacin controlled release. Journal of Polymer Engineering, 2013, 33, 659-664.	0.6	6
107	Preparation and Characterization of Magnetic Chitosan Microcapsules. Journal of Chemistry, 2013, 2013, 1-8.	0.9	9
108	Orientation-specific responses to sustained uniaxial stretching in focal adhesion growth and turnover. Proceedings of the National Academy of Sciences of the United States of America, 2013, 110, E2352-61.	3.3	73

#	Article	IF	CITATIONS
109	Measuring collective cell movement and extracellular matrix interactions using magnetic resonance imaging. Scientific Reports, 2013, 3, 1879.	1.6	10
110	Improvement in hemocompatibility of chitosan/soy protein composite membranes by heparinization. Bio-Medical Materials and Engineering, 2012, 22, 143-150.	0.4	7
111	Facile preparation of robust and biocompatible chitin aerogels. Journal of Materials Chemistry, 2012, 22, 5801.	6.7	163
112	Cellulose nanowhiskers: Preparation, characterization and cytotoxicity evaluation. Bio-Medical Materials and Engineering, 2012, 22, 121-127.	0.4	50
113	The 4th China–France Biotherapy and Regenerative Medicine International Symposium 2011. Bio-Medical Materials and Engineering, 2012, 22, 1-2.	0.4	0
114	Magnetic manipulation of actin orientation, polymerization, and gliding on myosin using superparamagnetic iron oxide particles. Nanotechnology, 2011, 22, 065101.	1.3	6
115	Soy protein-based polymer nanocomposites. , 2011, , 261-282.		0
116	Improvement in physical properties and cytocompatibility of zein by incorporation of pea protein isolate. Journal of Materials Science, 2010, 45, 6775-6785.	1.7	23
117	Properties and structural characterization of oxidized starch/PVA/αâ€zirconium phosphate composites. Journal of Applied Polymer Science, 2010, 115, 1089-1097.	1.3	47
118	Oxidized pea starch/chitosan composite films: Structural characterization and properties. Journal of Applied Polymer Science, 2010, 118, 3082-3088.	1.3	24
119	Creation of Hydrophobic Materials Fabricated from Soy Protein and Natural Rubber: Surface, Interface, and Properties. Macromolecular Materials and Engineering, 2010, 295, 451-459.	1.7	24
120	Preparation and characterization of chitosan/αâ€zirconium phosphate nanocomposite films. Polymer International, 2010, 59, 923-930.	1.6	47
121	Starch-based nanocomposites reinforced with layered zirconium phosphonate. Polymer Composites, 2010, 31, 1938-1946.	2.3	18
122	Preparation, Characterization, and <i>In Vitro</i> and <i>In Vivo</i> Evaluation of Cellulose/Soy Protein Isolate Composite Sponges. Journal of Biomaterials Applications, 2010, 24, 503-526.	1.2	38
123	Effects of starch nanocrystalâ€ <i>graft</i> â€polycaprolactone on mechanical properties of waterborne polyurethaneâ€based nanocomposites. Journal of Applied Polymer Science, 2009, 111, 619-627.	1.3	20
124	The transmembrane protein CBP plays a role in transiently anchoring small clusters of Thy-1, a GPI-anchored protein, to the cytoskeleton. Journal of Cell Science, 2009, 122, 3966-3972.	1.2	51
125	The synergetic bone-forming effects of combinations of growth factors expressed by adenovirus vectors on chitosan/collagen scaffolds. Journal of Controlled Release, 2009, 136, 172-178.	4.8	59
126	Thermoforming starchâ€ <i>graft</i> â€polycaprolactone biocomposites via oneâ€pot microwave assisted ring opening polymerization. Journal of Applied Polymer Science, 2009, 113, 2973-2979.	1.3	27

#	Article	IF	CITATIONS
127	Pea starchâ€based composite films with pea hull fibers and pea hull fiberâ€derived nanowhiskers. Polymer Engineering and Science, 2009, 49, 369-378.	1.5	66
128	Hypoglycemic effects of malonylâ€ginsenosides extracted from roots of <i>Panax ginseng</i> on streptozotocinâ€induced diabetic mice. Phytotherapy Research, 2009, 23, 1426-1430.	2.8	38
129	Bionanocomposites based on pea starch and cellulose nanowhiskers hydrolyzed from pea hull fibre: Effect of hydrolysis time. Carbohydrate Polymers, 2009, 76, 607-615.	5.1	339
130	Structure and properties of starch/α-zirconium phosphate nanocomposite films. Carbohydrate Polymers, 2009, 77, 358-364.	5.1	59
131	Rubiacordone A: A New Anthraquinone Glycoside from the Roots of Rubia cordifolia. Molecules, 2009, 14, 566-572.	1.7	25
132	Soy proteinâ€based nanocomposites reinforced by supramolecular nanoplatelets assembled from pluronic polymers/β yclodextrin pseudopolyrotaxanes. Journal of Applied Polymer Science, 2008, 107, 409-417.	1.3	10
133	Structure and mechanical properties of cellulose derivatives/soy protein isolate blends. Journal of Applied Polymer Science, 2008, 107, 3267-3274.	1.3	38
134	Green composites reinforced with hemp nanocrystals in plasticized starch. Journal of Applied Polymer Science, 2008, 109, 3804-3810.	1.3	202
135	Comparative study on the films of poly(vinyl alcohol)/pea starch nanocrystals and poly(vinyl) Tj ETQq1 1 0.7843	314 rgBT /(Dverlock 10 T
136	Structural characterization and properties of starch/konjac glucomannan blend films. Carbohydrate Polymers, 2008, 74, 946-952.	5.1	103
137	Physical properties and biocompatibility of cellulose/soy protein isolate membranes coagulated from acetic aqueous solution. Journal of Biomaterials Science, Polymer Edition, 2008, 19, 479-496.	1.9	31
138	Structure and Properties of Soy Protein/Alumina Hydrate Nanocomposites Fabricated via <i>In Situ</i> Synthesis. Journal of Biobased Materials and Bioenergy, 2008, 2, 248-257.	0.1	10
139	Three-dimensional Nanohydroxyapatite/Chitosan Scaffolds as Potential Tissue Engineered Periodontal Tissue. Journal of Biomaterials Applications, 2007, 21, 333-349.	1.2	50
140	pHâ€sensitive alginate/soy protein microspheres as drug transporter. Journal of Applied Polymer Science, 2007, 106, 1034-1041.	1.3	44
141	Preparation and properties of plasticized starch/multiwalled carbon nanotubes composites. Journal of Applied Polymer Science, 2007, 106, 1431-1437.	1.3	78
142	A New Network Composite Material Based on Soy Dreg Modified with Polyurethane Prepolymer. Macromolecular Materials and Engineering, 2007, 292, 484-494.	1.7	12
143	Direct interaction with filamins modulates the stability and plasma membrane expression of CFTR. Journal of Clinical Investigation, 2007, 117, 364-374.	3.9	85
144	STAT6 specific shRNA inhibits proliferation and induces apoptosis in colon cancer HT-29 cells. Cancer Letters, 2006, 243, 38-46.	3.2	32

#	Article	IF	CITATIONS
145	Methods to measure the lateral diffusion of membrane lipids and proteins. Methods, 2006, 39, 147-153.	1.9	135
146	Properties and biodegradability of water-resistant soy protein/poly(É-caprolactone)/toluene-2,4-diisocyanate composites. Polymer Degradation and Stability, 2006, 91, 2189-2197.	2.7	36
147	Toughened composites prepared from castor oil based polyurethane and soy dreg by a one-step reactive extrusion process. Journal of Applied Polymer Science, 2006, 101, 953-960.	1.3	9
148	Role of Star-Like Hydroxylpropyl Lignin in Soy-Protein Plastics. Macromolecular Materials and Engineering, 2006, 291, 524-530.	1.7	52
149	Transient anchorage of cross-linked glycosyl-phosphatidylinositol–anchored proteins depends on cholesterol, Src family kinases, caveolin, and phosphoinositides. Journal of Cell Biology, 2006, 175, 169-178.	2.3	83
150	Simultaneous Stretching and Contraction of Stress Fibers In Vivo. Molecular Biology of the Cell, 2004, 15, 3497-3508.	0.9	176
151	Transient confinement zones: A type of lipid raft?. Lipids, 2004, 39, 1115-1119.	0.7	32
152	Preparation and properties of water-resistant soy dreg/benzyl konjac glucomannan composite plastics. Journal of Applied Polymer Science, 2004, 91, 2061-2061.	1.3	3
153	Blend membranes prepared from cellulose and soy protein isolate in NaOH/thiourea aqueous solution. Journal of Applied Polymer Science, 2004, 94, 748-757.	1.3	30
154	Preparation and properties of water-resistant soy dreg/benzyl konjac glucomannan composite plastics. Journal of Applied Polymer Science, 2003, 90, 3790-3796.	1.3	27
155	Structure and Properties of Composites Compression-Molded from Polyurethane Prepolymer and Various Soy Products. Industrial & Engineering Chemistry Research, 2003, 42, 6786-6794.	1.8	47
156	c-Jun NH2-terminal Kinase Activation Leads to a FADD-dependent but Fas Ligand-independent Cell Death in Jurkat T Cells. Journal of Biological Chemistry, 2001, 276, 8350-8357.	1.6	37